Published in final edited form as:
Skin Res Technol. 2011 November ; 17(4): 387–397. doi:10.1111/j.1600-0846.2011.00508.x.

Characterization and quantification of wound-induced hair follicle neogenesis using *in vivo* confocal scanning laser microscopy

Chengxiang Fan[1], **Michael A. Luedtke**[2], **Stephen M. Prouty**[3], **Michelle Burrows**[4], **Nikiforos Kollias**[2], and **George Cotsarelis**[4]

[1] Drexel University, School of Biomedical Engineering, Science & Health Systems, Philadelphia, PA, USA

[2] Johnson & Johnson Consumer and Personal Products Worldwide, Models and Methods Skillman, NJ USA

[3] Follica, Inc. Philadelphia VA Medical Center, Bldg 21, 3900 Woodland Avenue, Philadelphia, PA USA

[4] University of Pennsylvania School of Medicine, Philadelphia, PA USA

Abstract

Background—*In vivo* confocal scanning laser microscopy (CSLM) is a recently-developed non-invasive technique for visualizing microscopic structures with the skin. CSLM has been used to characterize proliferative and inflammatory skin diseases, neoplastic skin lesions and pigmented lesions.

Objective—Here, we assessed the ability of CSLM to evaluate the formation of neogenic hair follicles after a full thickness wound in mice.

Methods—Full-thickness wounds were made on the dorsal skin of 3-week old mice. After scab detachment (SD), the number, width, length, space and volume of neogenic hair follicles were analyzed using CSLM. The results were compared with those from conventional methods, including staining for alkaline phosphatase (AP) and keratin 17 (K17) as well as histology.

Results—Quantification of neogenic hair follicles using CSLM compared favorably with results from direct measurements on isolated epidermal tissue after immunostaining for K17, a marker for the epithelial portion of new hair follicles. CSLM detected 89% of K17-stained follicles. CSLM more accurately quantitated the number of new follicles compared to AP staining, which detects the dermal portion of the new follicle. The width and length measurement from CSLM and histology were very close and correlated with each other. The minimum length of a neogenic hair follicle that could be detected by CSLM was 21 μm. The space between neogenic hair follicles was decreased in histological sections compared to CSLM.

Conclusions—CSLM is an accurate and valuable method for counting and measuring neogenic hair follicles non-invasively. CSLM produces images similar to histology in mice. Measurements of microstructures using CSLM more accurately reflect actual sizes since this technique avoids fixation artifact. In vivo visualization of developing follicles with CSLM permits detection of serial changes in hair follicle formation, thus conserving numbers of mice required for studies and improving detection of temporal changes in developing hair follicles.

Correspondence to: George Cotsarelis.

Keywords

Confocal scanning laser microscopy (CSLM); *In vivo* confocal microscopy (IVCM); reflectance confocal microscopy (RCM); hair follicle neogenesis (HFN); medical imaging; non-invasive imaging; wound healing; wound-induced hair follicle neogenesis (WIHN); alkaline phosphatase (AP); keratin 17 (K17); histology; full-thickness excision (FTE); epidermis; dermis

Introduction

New hair follicles develop during wound healing in the adult rabbit (1, 2), mouse (3), and possibly human (4). Lineage analysis using traceable genetic alterations in transgenic mice indicates that interfollicular epidermal cells in the wound assume a hair follicle lineage and generate new hair follicles (5). Spatiotemporal monitoring of this process has the potential to improve our understanding of this phenomenon, and ultimately to provide more detailed information for evaluating the response of neogenic hair follicles to therapeutic modulation.

Several imaging technologies are used to image skin in basic and clinical dermatological research. These include surface microscopy, high-frequency ultrasound (HFUS), laser Doppler perfusion imaging (LDPI), magnetic resonance imaging (MRI) and *in vivo* confocal scanning laser microscopy (CSLM) (6, 7). Among these techniques, CSLM provides the highest resolution imaging of the epidermis, reticular and upper papillary dermis (8).

CSLM was invented by Marvin Minsky at Harvard University in 1957 (9, 10). By using a point source of light and placing a pinhole in an optically conjugate plane in front of a photodetector, only the light from the single in-focus plane is collected. This approach eliminates light from out-of-focus planes thus greatly improving image quality compared with a wide-field microscope (11). Later, the confocal scope was adapted to image human skin and cornea *in vivo* (12–15). In 1995, a video-rate CSLM was developed (16).The CSLM used in the current study (Vivascope 1500, Lucid Inc., Rochester, NY) is a class II medical device occasionally used in dermatological practices as a means to noninvasively image and diagnose skin lesions.

In CSLM, the visualization of skin structures is based on the refractive index differences of the organelles and other microstructures from the background (9, 17, 18). Melanin (19), collagen (20) and keratin (21), which have high-refractive indices, produce strong back scatter with visible and near infrared wavelengths and thus function as good natural contrast reagents in the skin (7).

CSLM produces horizontal, or *en face*, optical sections less than 5 μm in thickness with a lateral resolution of 0.5–1.0 μm (22), thus providing images of the cellular layer and the upper dermal region of the skin. Maximal depth visualized with CSLM nears 350 μm, so generally structural and functional changes of human skin from stratum corneum (SC) to papillary dermis or even upper reticular dermis can be visualized. Interpolation of discrete optical sections produces continuous qualitative three-dimensional images and quantitative measures of tissue. To date, CSLM has been used to characterize proliferative and inflammatory skin diseases, neoplastic skin lesions and pigmented lesions (8).

This study was designed to show the feasibility of using CSLM to monitor the regeneration of hair follicles during wound healing following a full thickness cutaneous excision. We have termed this phenomenon “Wound-Induced Hair Follicle Neogenesis” or WIHN (5). In this study, we quantified several parameters of WIHN using CSLM, including number, width, length and volume of the new follicles. The thickness of the SC and viable epidermis

were measured as well. These results were compared and analyzed in correlation with other conventional methods including alkaline phosphatase (AP) staining, Keratin 17 (K17) staining and histology. The dynamic changes of neogenic hair follicles over time in the same animal were also evaluated by CSLM.

Materials and Methods

Confocal imaging

A commercially available CSLM (Vivascope 1500, Lucid Inc., Rochester, NY) was used. A detailed description of this system has been published (16, 22). This microscope uses an 830 nm Nichia diode laser operating at a power less than 20 mW as measured at the output of the objective. A 30× magnification 0.9 NA water immersion objective was used.

A small drop of high index of refraction (n=1.5) oil (Crodamol CGS, Croda NJ) was placed on the surface of a wound to match the index of refraction of the stratum corneum in order to increase visibility of hair follicles. The placement of a metallic tissue ring holder together with a disposable 30 mil medical grade adhesive polycarbonate window (Lucid, USA) onto the wound and surrounding fur creates a secure well for holding the water-based immersion medium. A drop of ultrasound transmission gel immersion media (AquasonicR, Parker Laboratories, Inc. USA) was applied inside the tissue ring on the surface of the window. The CSLM imaging module was attached to the tissue ring magnetically. Using this *in vivo* method the tissue can be translated relative to the objective lens of CSLM in a controlled manner. A VivaCube program was configured to acquire eight 8mm × 8mm VivaBlock images at 20 μm depth intervals relative to the tissue surface. Then at least 3 replicate 0.5mm × 0.5mm Vivastack images were acquired within the 8×8mm region at 1.473 μm depth intervals to a 200 μm depth to allow for skin thickness measurements.

Animals and treatments

In total, 26 C57Bl/6J mice were ordered from The Jackson Laboratory. These mice were treated in accordance with NIH guidelines and all relevant animal protocols were approved by the University of Pennsylvania Institutional Animal Care and Use Committee (IACUC).

Correlation of hair follicle counts between CSLM, AP, and K17 assays

11 mice, 21 days old, were weighed and anesthetized with ketamine/xylazine, and the dorsal fur clipped. A 1 cm^2 square of full-thickness dorsal skin was excised using surgical scissors and forceps. On Days 5–9 after scab detachment (SD), CSLM images were taken on the wound areas. The wound skin was harvested and incubated in 20 mM EDTA/PBS solution at 37oC overnight. With fine tweezers, the epidermis was separated from the dermis under a dissecting microscope. The dermis was processed for AP staining and the epidermis for K17 staining as described below.

AP staining—The dermis was fixed in acetone for 1–2 days. Then, it was rinsed with phosphate buffered solution (PBS) and Genius III solution successively. The sample was incubated with AP substrate, which is made up of 0.375 mg/ml nitro blue tetrazolium chloride (NBT) and 0.188 mg/ml 5-bromo-4-chloro-3-indolyl phosphate (BCIP) (Roche Diagnostics GmbH, Germany), at 37 °C for 15 minutes. After being rinsed with 25 mM EDTA solution (Boston BioProducts, USA), it was stored in water for later analysis.

K17 staining—The epidermis was fixed in 10% formalin solution at room temperature for 1 hour and then incubated with 3% hydrogen peroxide solution (Fisher Scientific, USA). After being blocked with 5% BSA solution (Fisher Scientific, USA), the sample was incubated with K17 antibody (1:5000) (courtesy of Dr. Pierre Coulombe, John Hopkins

University) and then biotinylated anti-rabbit IgG (1:200) (Vector Laboratories, Inc.) followed by Streptavidin Horseradish Peroxidase (HRP) (1:500) (CALBIOCHEM, USA). Finally, it was incubated in diaminobenzidine (DAB) solution (Sigma, USA) for 5 minutes.

Resulting histology samples were digitally imaged with a dissecting microscope. Confocal Vivablock images were captured with respect to the orientation of the mouse. Quantitative measures of these images were analyzed using Image J. Each sample was counted twice and the final result was the average of the replicate measures.

The relative orientation of the microscope on the mouse as well as the orientation of the tissue sample needed to be synchronized with great care. The K17 images were flipped vertically in order to match their orientation with AP and confocal images. This was necessary for direct correlation between the different methods.

Measurement of hair follicle length and viable epidermal thickness by CSLM and its comparison with histology

Seven 21 day old mice were wounded as described above. Using 1 mouse per day from day 1 through 7 after SD, the wound was imaged with CSLM. A series of VivaStack images were acquired at intervals of 1.473 μm to a depth of ~200μm. After imaging, the wound was harvested and fixed in 10% neutral-buffered formalin (Fisher Scientific, USA) with a piece of notecard applied to the base of the specimen to prevent curling and missalignment during fixation. The fixed specimens were bisected and then transferred to 70% ethyl alcohol (Pharmaco Products Inc. USA). They were embedded in paraffin and sectioned vertically at 5 μm. Finally, these samples were stained with hematoxylin and eosin (H&E) (Surgipath Medical Industries Inc. USA). The classification of germ stages in this study is according to the guideline provided by Paus (23).

Quantification of the number, width and space of neogenic hair follicles by CSLM and its correlation with histology

Five mice were wounded as before. On Day 5 after SD, these mice were anesthetized, the wound was marked with India ink and then imaged using CSLM. Vivacube images were collected. Then, the same exact corresponding wounds were removed and placed between two glass slides secured with a rubber band with great care taken to note relative orientation of the tissue sample as it was acquired on the mouse. The CSLM was always attached to the mouse and oriented so that the head of the mouse was towards the upper portion of the screen. This was an important factor for allowing exact correlation of the CSLM images to histology. These samples were formalin fixed, embedded in paraffin wax, sectioned horizontally and stained with H&E.

To quantify neogenic hair follicles, horizontal histological sections and corresponding CSLM optical sections at the same depth were compared. The results from these two assays were collected and analyzed as indicated below.

Serial observation of neogenic hair follicle development in the same animal

Three mice were imaged using CSLM from Day 1 to Day 8 after SD. The same regenerating areas were retrieved from each cube file. Using these CSLM images, the same wound site was evaluated over time. The dynamic changes in the number, width and length of neogenic hair follicles were monitored. Once the number, and the average width and length of neogenic hair follicles in a mouse were determined, the volume of a model neogenic hair follicle was calculated according to the formula $v = 3.14 * (w/2)^2 * l$, where v is the volume of a model germ; w and l are the width and length of the neogenic hair follicle, respectively.

Morphometric analysis

For CSLM analysis, all parameters were obtained from collected images. The measurements on the X–Y level were done using the built-in software. The depth of each image was obtained by reading the calibrated depth (Z-axis) micrometer and the respective depth of the optical plane.

All parameters in the histological analysis were acquired from horizontal or vertical sections at 40× magnification under a microscope with a reticule. The number of ocular divisions spanned by a neogenic hair follicle was recorded and converted into length by being multiplied by a conversion factor, which is determined from the measurement of a stage micrometer. The microscope measurement system was calibrated in advance by a technology specialist from the Olympus Company.

For the quantification of neogenic hair follicles, each layer of CSLM cube images was counted using Image J. The layer with the most neogenic hair follicles was chosen and counted again. The final result was the average of these two counts. Similarly, the neogenic hair follicles in the histological slides were examined and counted.

For confocal length measurement, a series of CSLM stack images were examined from the surface of skin to deep tissue. Fig. 1 shows a diagram illustrating the length measurement in CSLM analysis. Similarly, the thickness of SC and viable epidermis were also measured (Fig. 2). In histology, these measurements were made directly under an optical microscope as described above.

In CSLM images, the width and distance between hair follicles were measured using the built-in Line Measurement Tool in the VivaScan Software (Version 7.0). The width is the distance from one edge of the hair follicle to the other along the smallest dimension. The space between hair follicles is the distance from the center of one neogenic hair follicle to the center of the neighboring one. The width and space measurements for histology sections were accomplished in a similar way under a light microscope with a reticule.

Statistical methods

Data are reported as mean ± standard deviation (SD). T-test and correlation analysis were conducted using Prism 4 (version 4.03, GraphPad Software, Inc.). All tests were two-tailed. The statistical significance was determined at $P < 0.05$.

Results

Correlation of hair follicle counts between CSLM, AP-staining, and K17-staining assays

In confocal images, neogenic hair follicles are shown as circular structures of different diameters, with a well-circumscribed border. A cube of 8 layers was produced and all layers were counted and compared. The layer with the most neogenic hair follicles was reported, which is usually the 4th layer of the cube images. This layer is about 60 μm below the skin surface, and it is just generally at the level of the papillary dermis. The distribution pattern of the neogenic hair follicles in the resulting CSLM images match with K17 and AP staining (Fig. 3a).

For the quantification of neogenic hair follicles, K17 immunohistochemical staining visualizes the highest number of neogenic hair follicles for each sample. The confocal method is the second most sensitive method, visualizing 89% of the hair follicles detected by K17 staining. AP staining detects the fewest number of hair follicles with 69% as many as the K17 assay. Both the AP staining and the confocal counts significantly correlate with the K17 assay ($P<0.0002$ and $P<0.001$ respectively). The confocal count correlates well with

K17 staining with a correlation coefficient of 0.99. In contrast, the correlation coefficients for AP-confocal and AP-K17 are 0.77 and 0.81, respectively (Fig. 3b).

Comparison of hair follicle length and viable epidermal thickness measurements obtained by CSLM and histology

For two of the seven mice in this group, the histology sample was incomplete, making it difficult to make a comparison with CSLM. Therefore, only 5 samples were quantified and analyzed.

After scab detachment (SD), the wounded area begins to regenerate hair follicles. These neogenic hair follicles appear to form asynchronously. Different stages of neogenic hair follicles, from pre-germ to more advanced hair follicles, can be seen within one section (Fig. 4a). From Day 1 to Day 7 after SD, neogenic hair follicles from stage 0 until stage 5 appear. Fig. 4b shows histology of some representative neogenic hair follicles in different stages.

In confocal analysis, the length of the neogenic hair follicles was assessed by analyzing the sequential CSLM stack images. The results correlate well with those from the histological analysis. Even though the ranges in length differ, there are no significant differences between the two kinds of measurements ($P>0.05$; Fig. 5a). From the data obtained in this study, the minimum length that can be detected by CSLM is 21 μm, which is the early stage of S_2 germ. The measurement of the viable epidermal thickness from CSLM also correlated well with that from the histological analysis (Fig. 5b).

Quantification of the number, width and space of neogenic hair follicles using CSLM: comparison to histology

For quantification of neogenic hair follicles, results from CSLM images and histological horizontal sections correlated well with each other (Fig. 6a). The distribution patterns of these neogenic hair follicles in both images were very similar. Fig. 6c shows a representative match between CSLM images and histology sections.

The width measurements were taken in both confocal and histological *en face* images. Overall, the results from both methods were very similar (Fig. 6b). Measurements of specific neogenic hair follicles from a representative pair of confocal and histological images were also compared. The width measurements from both assays were very close (100.0 vs. 101.5). Space analysis, however, showed approximately a 6% decrease in space measurement from the histological section compared with that from corresponding confocal image data (100.0 vs. 93.6) (Fig. 6d).

Serial observation of the development of neogenic hair follicles in the same mouse

The dynamic change of the above parameters can be demonstrated clearly by performing CSLM on the same mouse over a period of time (Fig. 7). One day after SD, prominent vascular networks were detected in the central part of the wound in which the neogenic hair follicles will develop later. This suggests that the wounds are highly metabolic, even though no germs can be seen at this time. From Day 2, some pre-germs can be detected in the central part of the wound, in close proximity to small blood vessels. By Day 3, neogenic hair follicles can clearly be seen. Later on, these neogenic hair follicles continue to increase in number and length. In contrast, the thickness of the viable epidermis decreases over time. The width of hair follicles remains relatively stable after formation (Fig. 8a & b). The volume of the model germ also increases with time (Fig. 8c).

Discussion

The normal wound healing process occurs in a predictable manner and involves the stages of hemostasis, inflammation and repair (24). *De novo* hair follicle formation occurs several days after reepithelialization (5). Previous lineage analysis indicates that new follicles arise from epidermal cells outside of the bulge cell area (5). Following the formation of new hair follicles serially in the same mouse improves the ability to study this regenerative phenomenon. Here we show that CSLM is a valuable technique for this purpose.

In studying WIHN, the number of neogenic hair follicles is an important parameter. To visualize neogenic hair follicles in tissue samples, we previously stained for K17 protein and AP activity in wholemount preparation of epidermis and dermis, respectively. AP is an enzyme expressed by hair follicle dermal papilla and K17 is an intermediate filament protein and a hair follicle differentiation marker expressed during hair follicle development and in adult follicle outer root sheath (28). Thus, K17 immunostaining is an excellent method for detecting neogenic hair follicles in this full-thickness excision (FTE) wound model as it can detect very early stages of neogenic hair follicles. It is not surprising that this assay results in the visualization of the highest number of neogenic hair follicles for each sample.

In contrast to K17 staining, AP staining, on average, results in detection of fewer neogenic hair follicles. AP staining is based on the AP activity of cells within the dermal condensate of neogenic hair follicles (23, 29). The dermal condensates associated with hair germs in early to middle stages of development tend to be well stained. Dermal condensates in the later stages tend not to stain well. Likely, this is because during late stages of hair follicle development these cells are deeper in the dermis in areas where the AP substrate has more difficulty penetrating. In addition, in whole mount samples, the hair follicle dermal condensates and papillae are not always clearly seen since they lie at the bottom of the hair follicle sheath. These factors likely collectively contribute to the low number of the AP staining method.

CSLM detects neogenic hair follicles in intact skin without a need for processing the tissue. In comparing CSLM to previous invasive means for quantitating hair follicle neogenesis, our results showed that CSLM was more accurate than AP staining (89% vs. 69%, respectively in comparison to K17 staining) for detecting new hair follicles. The discrepancy between CSLM and K17 assays likely occurred because CSLM can not detect the hair germs at very early stages. In contrast, K17 staining even detects hair follicle placodes that form before the germ stage, therefore K17 staining remains the gold standard for quantitation of early hair germ structures.

The measurement of neogenic hair follicle length using CSLM is accomplished by analyzing the stack images. The neogenic hair follicle is a down-growth of densely packed keratinocytes surrounded by loose dermal connective tissue. Therefore hair germs are easily visualized as dark circular structures surrounded by brighter dermis. At later stages of development, melanin is associated with hair germs and it produces a very bright signal. Additionally, in some developing hair follicles at slightly later stages, the hair follicle dermal papilla and its associated capillary loop can be clearly visualized. For measurement of neogenic hair follicle length, the most important parameters are Z_0 and Z_x layers (Fig. 1). The changes between layers are subtle, but these two layers can still be accurately identified after careful comparison with adjacent layers.

In human epidermis, CSLM allows for measurement of epidermal thickness since specific layers of epidermis can be detected (22).We found that mouse epidermal thickness can also be measured. Once the top of the granule cell layer and the bottom of the basal layer are

determined, the thickness of viable epidermis can be calculated. We found that measurements from CSLM correlated well with measurements from histology (Fig. 5).

The confocal images also correlate well with horizontal histological sections. The number, as well as the pattern of neogenic hair follicles in both images matched well (Fig. 6a&c). In particular results of the width measurements from both assays were very close. However, there was more of a discrepancy from the space measurements. The space between neogenic hair follicles was smaller in histological sections compared to confocal images (Fig. 6c&d). Dehydration and shrinkage of the tissue during histological processing likely accounts for this. The hair follicle germs, which are composed of densely packed follicle epithelial cells, are less affected by this shrinkage. Thus, the width of the germs does not change much in the course of histological processing. In contrast, the inter-follicular tissue, being composed of connective tissue tends to be prone to dehydration and shrinkage. It is well-known that tissue processing for paraffin embedding causes tissue shrinkage. Using CSLM, we found that this shrinkage is approximately 6 percent.

When correlating CSLM images to conventional histological images, the major difference is the orientation of sections (17, 18). For CSLM, images are produced horizontally to the skin surface (*en face*) whereas skin histology is usually sectioned in the vertical plan. In our study, skin was also sectioned horizontally in order to compare these two methods more directly. Because mouse skin is so thin, obtaining horizontal tissue sections for histology was challenging. Only 60% of slides contained acceptable images. The causes for failures include non-parallel skin surface when sectioning and a partial loss of sample during the tissue processing. For CSLM, a metal ring with a polymer window is attached to skin. The ring is then magnetically connected to the objective lens housing. This design decreases problems with orientation, and in this regard, CSLM has an obvious advantage over conventional histology.

In order to monitor the dynamic changes occurring over time during hair follicle neogenesis, the number, width and length of neogenic hair follicles were followed using CSLM. Both the number and length markedly increased over time, whereas the width increased slightly. To integrate all the dynamic information, we proposed the concept of a model germ. A model germ is a virtual germ representing the typical changes in the above parameters. In this model, the neogenic hair follicle is treated as a cylindrical object (Fig. 8c). The volume of a model germ can be calculated based on the above parameters. Similarly, the total volume of the neogenic hair follicles in a regenerating area can also be obtained, which represents all the neogenic hair follicles in each animal (data not shown). These indices might be useful in evaluating the responses of neogenic hair follicles to drugs or other therapeutic modulators. The dynamic *in vivo* information about these parameters offers a potential to increase our understanding of WIHN.

CSLM offers several important advantages over conventional methods for studying hair follicle neogenesis following wounding. For example, the same skin site can be imaged serially over time. CSLM images are collected directly from the tissue thus avoiding histological artifacts. Information regarding the number, length and width of neogenic hair follicles can be obtained from a single animal. Thus, these features can help to decrease the number of experimental animals used in an experiment.

Acknowledgments

We would like to thank Leroy Ash for his skilled technical assistance in histology. We are also grateful to Dave William for the calibration of the light microscope for measurement. This work was supported by Follica. Inc.

References

1. Billingham RE, Russell PS. Incomplete wound contracture and the phenomenon of hair neogenesis in rabbits' skin. Nature. 1956 Apr 28; 177(4513):791–2. [PubMed: 13321965]
2. Breedis C. Regeneration of hair follicles and sebaceous glands from the epithelium of scars in the rabbit. Cancer Res. 1954 Sep; 14(8):575–9. [PubMed: 13199800]
3. Lacassagne A, Latarjet R. Action of methylcholanthrene on certain scars of the skin in mice. Cancer Res. 1946; (6):183–8. [PubMed: 21018721]
4. Kligman AM, Strauss JS. The formation of vellus hair follicles from human adult epidermis. J Invest Dermatol. 1956 Jul; 27(1):19–23. [PubMed: 13357817]
5. Ito M, Yang Z, Andl T, Cui C, Kim N, Millar SE, et al. Wnt-dependent de novo hair follicle regeneration in adult mouse skin after wounding. Nature. 2007 May 17; 447(7142):316–20. [PubMed: 17507982]
6. Aspres N, Egerton IB, Lim AC, Shumack SP. Imaging the skin. Australas J Dermatol. 2003 Feb; 44(1):19–27. [PubMed: 12581077]
7. Astner S, Dietterle S, Otberg N, Rowert-Huber HJ, Stockfleth E, Lademann J. Clinical applicability of in vivo fluorescence confocal microscopy for noninvasive diagnosis and therapeutic monitoring of nonmelanoma skin cancer. J Biomed Opt. 2008 Jan–Feb.13(1):014003. [PubMed: 18315361]
8. Gonzalez S, Swindells K, Rajadhyaksha M, Torres A. Changing paradigms in dermatology: confocal microscopy in clinical and surgical dermatology. Clin Dermatol. 2003 Sep–Oct; 21(5): 359–69. [PubMed: 14678715]
9. Minsky, M. Microscopy apparatus. US Patent. 3013467. 1957 Nov 7.
10. Minsky M. Memoir on inventing the confocal scanning microscope. Scanning. 1988; 10:123–8.
11. McNally JG, Karpova T, Cooper J, Conchello JA. Three-dimensional imaging by deconvolution microscopy. Methods. 1999 Nov; 19(3):373–85. [PubMed: 10579932]
12. Webb RH, Hughes GW, Delori FC. Confocal scanning laser ophthalmoscope. Appl Opt. 1987; 26:8.
13. Bertrand C, Corcuff P. In vivo spatio-temporal visualization of the human skin by real-time confocal microscopy. Scanning. 1994; 16:150–4. [PubMed: 8038914]
14. Corcuff P, Leveque JL. In vivo vision of the human skin with the tandem scanning microscope. Dermatology. 1993; 186:50–4. [PubMed: 8435517]
15. Lemp MA, Dilly PN, Boyde A. Tandem scanning confocal microscopy of the full-thickness cornea. Cornea. 1985; 4:105–9.
16. Rajadhyaksha M, Grossman M, Esterowitz D, Webb RH, Anderson RR. In vivo confocal scanning laser microscopy of human skin: melanin provides strong contrast. J Invest Dermatol. 1995 Jun; 104(6):946–52. [PubMed: 7769264]
17. Huzaira M, Rius F, Rajadhyaksha M, Anderson RR, Gonzalez S. Topographic variations in normal skin, as viewed by in vivo reflectance confocal microscopy. J Invest Dermatol. 2001 Jun; 116(6): 846–52. [PubMed: 11407970]
18. Gonzalez S, Rajadhyaksha M, Anderson RR. Non-invasive (real-time) imaging of histologic margin of a proliferative skin lesion in vivo. J Invest Dermatol. 1998 Sep; 111(3):538–9. [PubMed: 9740254]
19. Vitkin IA, Woolsey J, Wilson BC, Anderson RR. Optical and thermal characterization of natural (Sepia officinalis) melanin. Photochem Photobiol. 1994 Apr; 59(4):455–62. [PubMed: 8022888]
20. Wang XMT, Chang M, Nelson J. Group refractive index measurement of dry and hydrated type I collagen films using optical low-coherence reflectometry. J Biomed Opt. 1996; 1:212–16.
21. Tearney G, Brezinski M, Southern JF, et al. Determination of the refractive index of highly scattering human tissue by optical coherence tomography. Opt Lett. 1995; 20(21):2258–60. [PubMed: 19862316]
22. Rajadhyaksha M, Gonzalez S, Zavislan JM, Anderson RR, Webb RH. In vivo confocal scanning laser microscopy of human skin II: advances in instrumentation and comparison with histology. J Invest Dermatol. 1999 Sep; 113(3):293–303. [PubMed: 10469324]

23. Paus R, Muller-Rover S, Van Der Veen C, Maurer M, Eichmuller S, Ling G, et al. A comprehensive guide for the recognition and classification of distinct stages of hair follicle morphogenesis. J Invest Dermatol. 1999 Oct; 113(4):523–32. [PubMed: 10504436]

24. Phillips SJ. Physiology of wound healing and surgical wound care. Asaio J. 2000 Nov–Dec; 46(6):S2–5. [PubMed: 11110286]

25. Cotsarelis G, Sun TT, Lavker RM. Label-retaining cells reside in the bulge area of pilosebaceous unit: implications for follicular stem cells, hair cycle, and skin carcinogenesis. Cell. 1990 Jun 29; 61(7):1329–37. [PubMed: 2364430]

26. Fuchs E. Scratching the surface of skin development. Nature. 2007 Feb 22; 445(7130):834–42. [PubMed: 17314969]

27. Gurtner GC, Werner S, Barrandon Y, Longaker MT. Wound repair and regeneration. Nature. 2008 May 15; 453(7193):314–21. [PubMed: 18480812]

28. McGowan KM, Coulombe PA. Onset of keratin 17 expression coincides with the definition of major epithelial lineages during skin development. J Cell Biol. 1998 Oct 19; 143(2):469–86. [PubMed: 9786956]

29. Iida M, Ihara S, Matsuzaki T. Hair cycle-dependent changes of alkaline phosphatase activity in the mesenchyme and epithelium in mouse vibrissal follicles. Dev Growth Differ. 2007 Apr; 49(3): 185–95. [PubMed: 17394597]

30. Selkin B, Rajadhyaksha M, Gonzalez S, Langley RG. In vivo confocal microscopy in dermatology. Dermatology Clinics. 2001; 19(2):369–77.

31. Luedtke MA, Papazoglou E, Neidrauer M, Kollias N. Wavelength effects on contrast observed with reflectance in vivo confocal laser scanning microscopy. Skin Res Technol. 2009 Nov; 15(4): 482–8. [PubMed: 19832962]

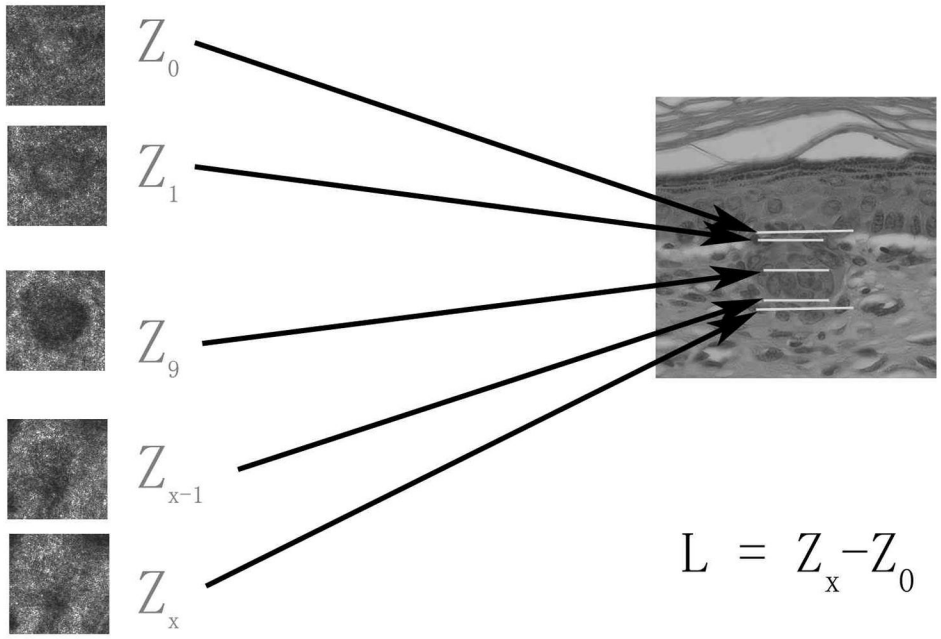

Figure 1. Length measurement from CSLM image analysis

Sequential stack images from SC to dermis were analyzed. Z_0 is defined as the deepest layer where the basal cells are observed, Z_1 is defined as the layer where the hair follicle germs are seen clearly, Z_{x-1} is the deepest layer where germs can still be seen and (Z_x) is defined as the layer where the germs are no longer observed. The depth information of these layers was obtained by normalizing the depth information relative to the stratum corneum surface and using the calibrated image steps from the skin surface. Once Z_0 and Z_x were determined,the length of the follicle (L) was calculated from the difference between these two layers.

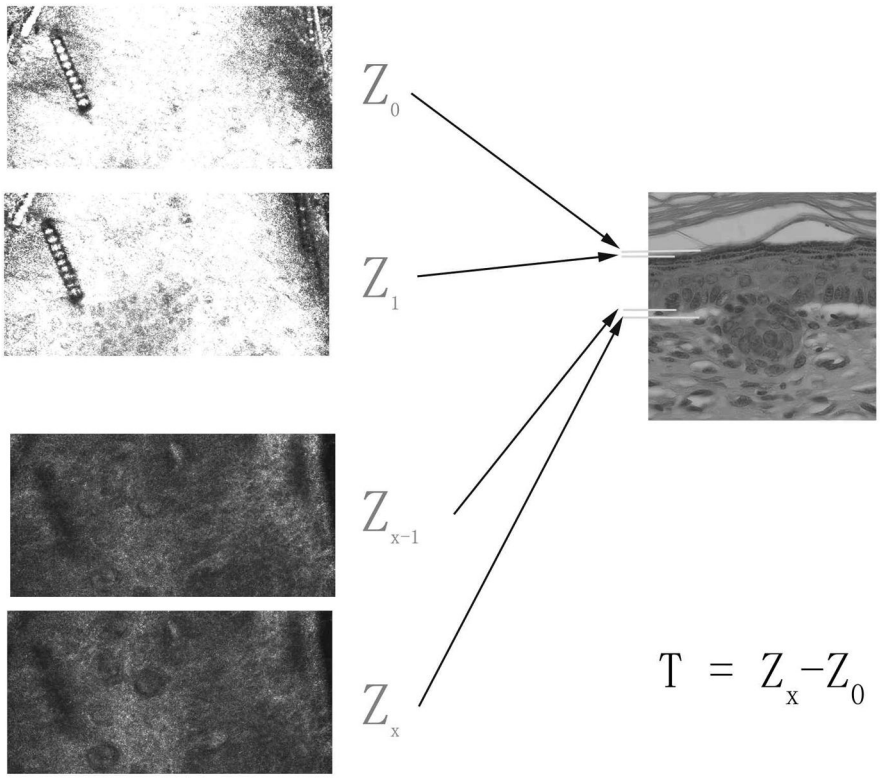

Figure 2. Thickness measurement of viable epidermis from CSLM image analysis

Sequential stack images from SC to dermis were analyzed. Z_0 is defined as the deepest layer where keratinocytes have not yet appeared, Z_1 is the layer where keratinocytes begin to appear, Z_{x-1} is defined as the last layer where basal cells are observed and Z_x is defined as the layer where the basal cells are no longer observed. The difference in depth between Z_x and Z_0 is defined as the thickness of viable epidermis (T).

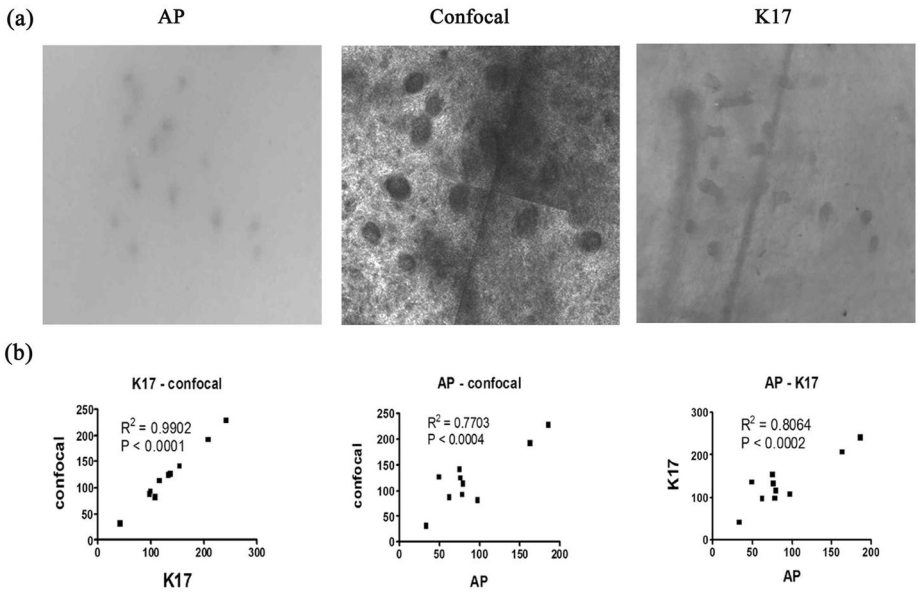

Figure 3. Correlation of neogenic hair follicle counts between AP, confocal and K17 assays

Fig. 3a) A representative match of AP, K17, and CSLM images used to quantify neogenic hair follicles. Fig. 3b) Demonstrates correlation analysis for the total counts of neogenic hair follicles between these assays.

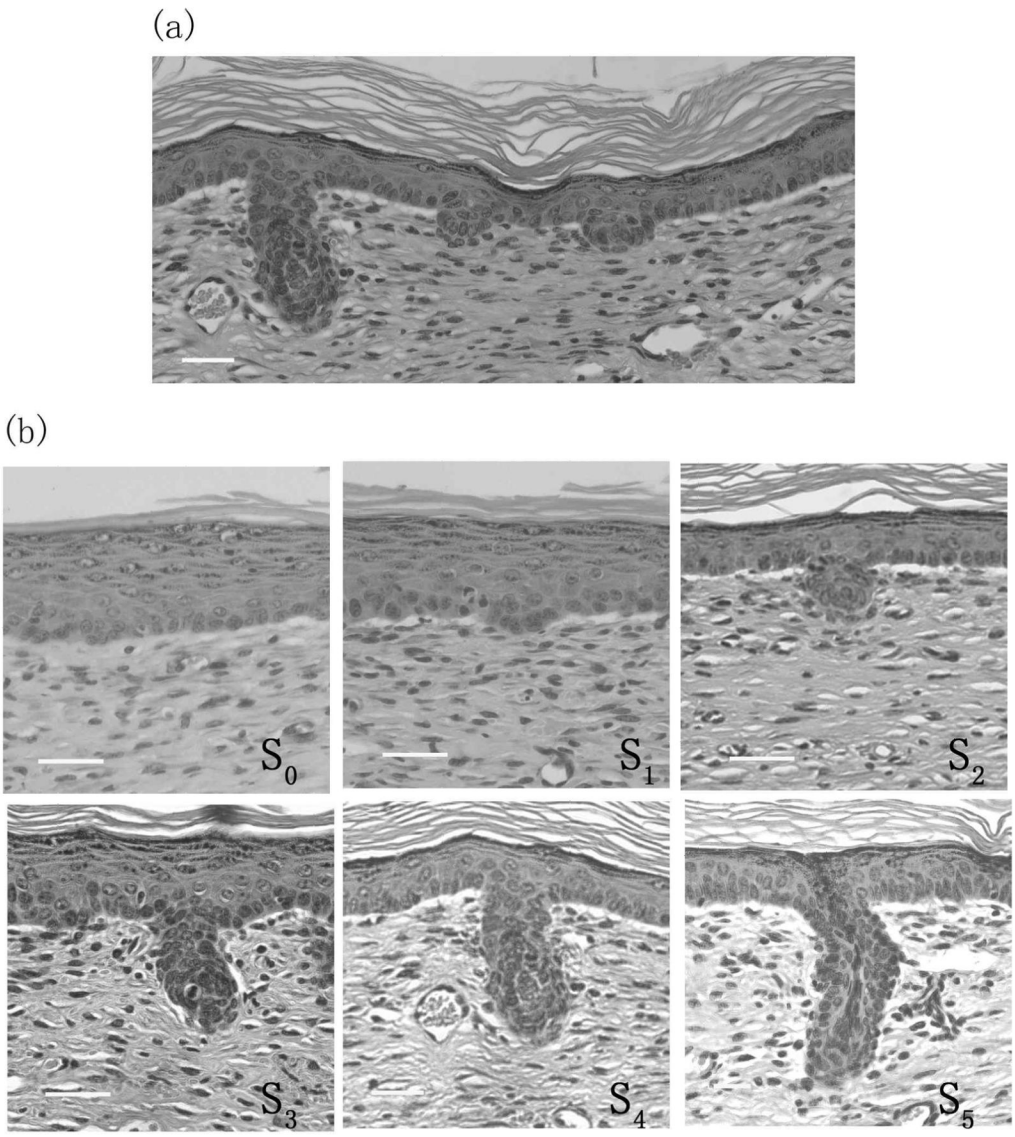

Figure 4. Different stages of neogenic hair follicles in the hair follicle neogenesis following wounding

Fig. 4a) shows the asynchrony of neogenic hair follicles. Different stages of neogenic hair follicles are seen in one sample after SD. Fig. 4b) shows representative neogenic hair follicles of different stages (S_0–S_5) seen at various times after SD. S_2 is the earliest germ detectable with CSLM. *Scale bar: 25 μm*

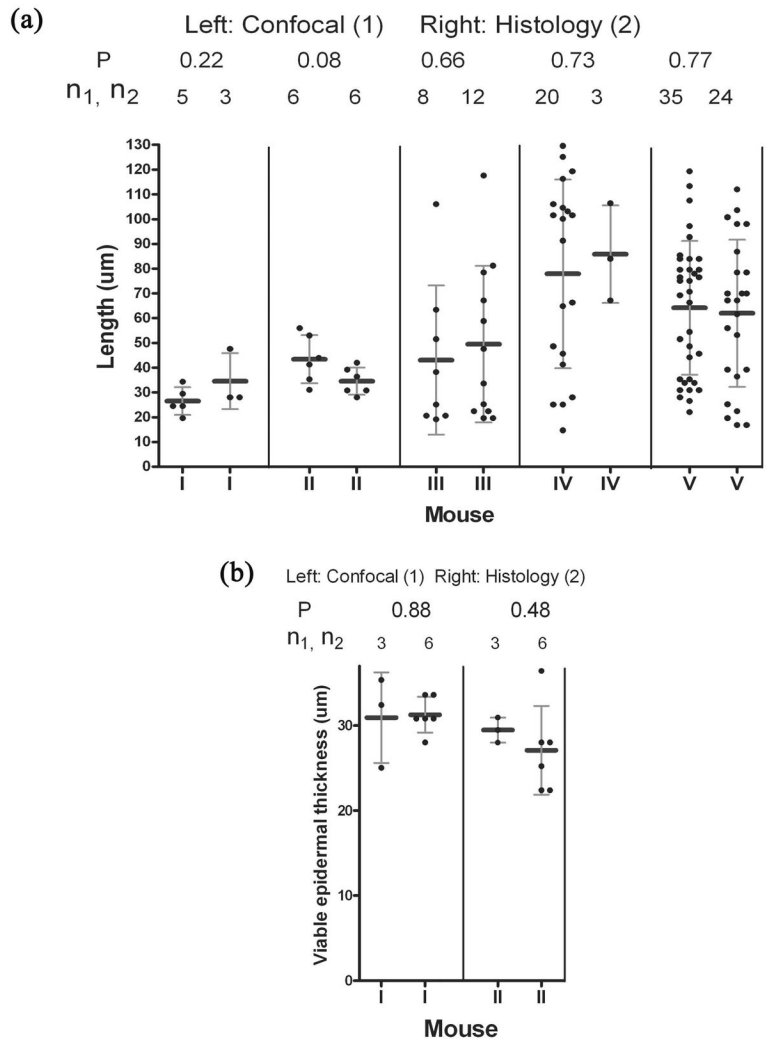

Figure 5. Comparison of length and viable epidermal thickness measurements between CSLM and histological methods

Fig 5a) shows the comparison of length measurement between CSLM and histology methods. Fig 5b) shows the results of viable epidermal thickness measurement from both methods. Measurements n_1 and n_2 are determined from confocal and histology methods respectively. P values are representative of the t-test of measurements from these two methods.

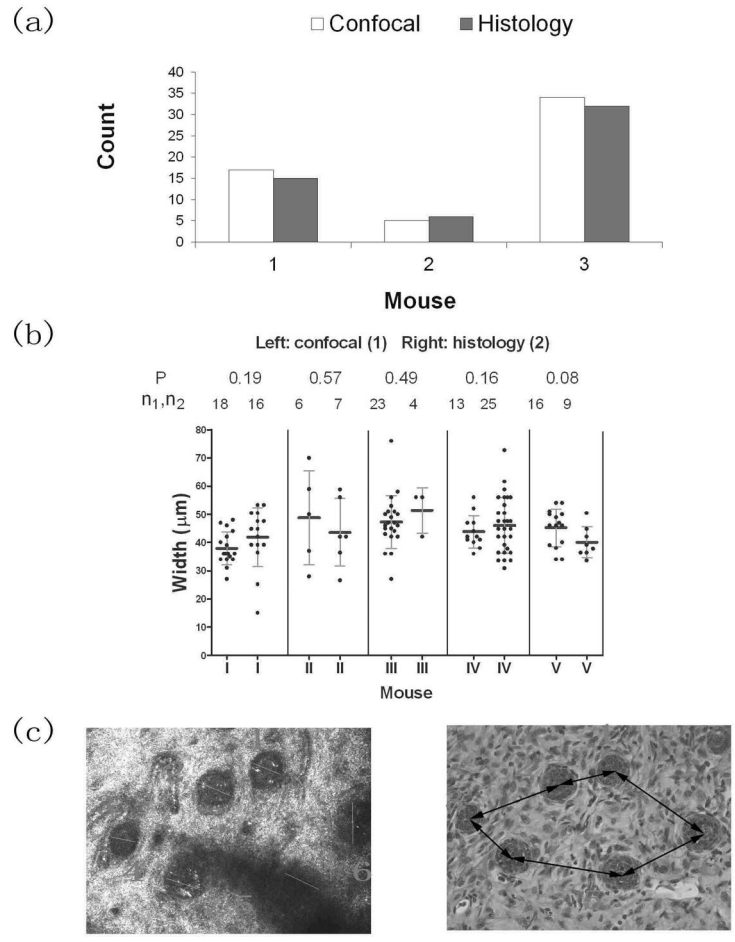

HF ID	Confocal image	Histological slide (μm)	Percentage (%)
1	44	49	111.4
2	52	56	107.7
3	38	39	103.2
4	56	53	95.0
5	61	56	91.8
6	56	56	100.0
Ave.			101.5 ± 7.0

Distance	Confocal image	Histological slide (μm)	Percentage (%)
1 to 2	82	78	95.6
2 to 3	155	134	86.7
3 to 4	108	83	76.5
4 to 5	173	151	87.4
5 to 6	117	126	107.7
6 to 1	143	157	109.7
Ave.			93.9 ± 13.0

Figure 6. Comparison of width and space measurements between CSLM and histological assays

Fig 6a) Total hair germ counts from confocal and histological assays. Fig. 6b) Comparison of width measurements between confocal and histological assays. Measurements n_1 and n_2 are from confocal and histology methods respectively. P values are representative of the t-test of measurements from these two methods. Fig. 6c) Is a representative match between CSLM and histological images. The confocal image (on left) also shows how width measurement was made, whereas the right histological image shows the space measurement. Fig 6d) shows the width and space analysis in the above pair of images.

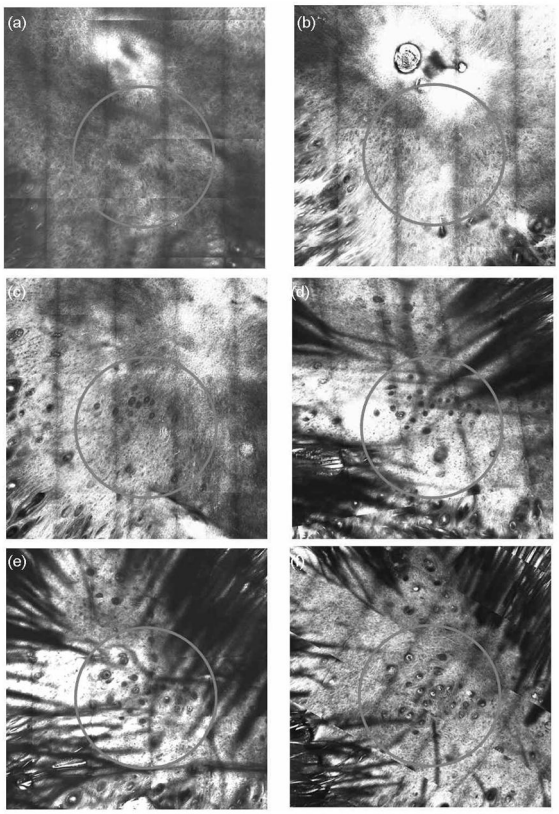

Figure 7. Development of neogenic hair follicles over time

The same mouse was imaged with CSLM from Day 1 to Day 8 after SD. The same regions were imaged each day. Figs. 7a, b, c, d, e and f show the wound areas of Day 1, 2, 3, 6, 7 and 8 after SD respectively.

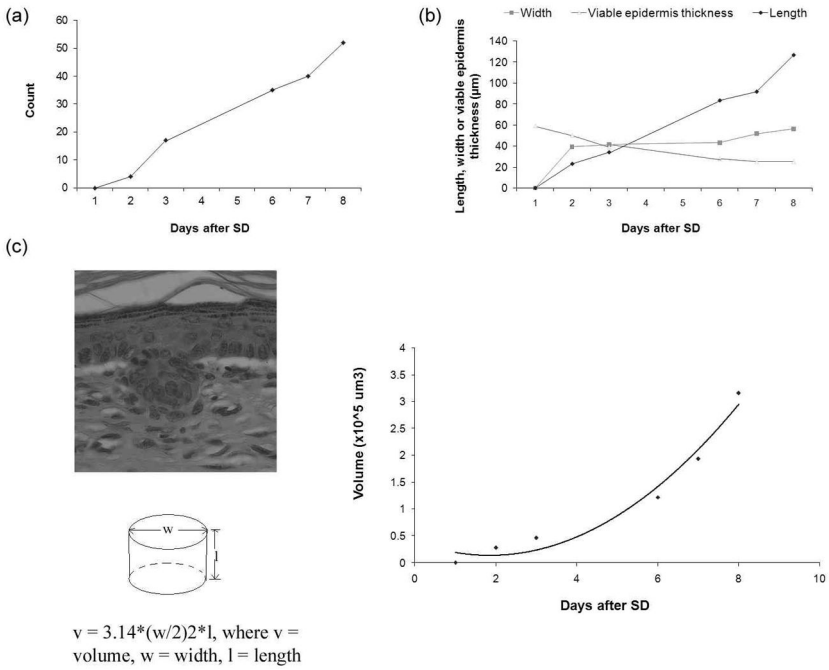

Figure 8. Dynamic changes of the parameters of neogenic hair follicles after SD

A mouse was imaged with CSLM from Day 1 through Day 8 after SD. Fig. 8a) demonstrates the dynamic change in the number of neogenic hair follicles. Fig. 8b) shows the dynamic changes in the length and width of neogenic hair follicles and thickness of viable epidermis. Fig 8c) Demonstrates the volume dynamics of a model neogenic hair follicle.